Mn DOPED CdS THIN FILMS BY USING CHEMICAL BATH DEPOSITION TECHNIQUE

Nalini
M.Phil Research Scholar, Post Graduate & Research Department of Physics
The American College, Madurai, India

S. Paul Mary Deborrah
Associate Professor, Post Graduate & Research Department of Physics
The American College, Madurai, India

Abstract

The transition metal Mn doped CdS have been synthesized by Chemical Bath Deposition method for various thickness of 1%, 2%, 5%. The Structure of the deposited Mn doped CdS was confirmed by Powder X-ray diffractometer. It has a main peak at 28.32° corresponding to the (2 4 0) plane. The Mn doped CdS thin films are found to be amorphous in nature. The UV-Vis-IR studies reveal that Mn doped CdS thin film was in the range of 200-900 nm. The Optical band gap was found to be 3.84 eV-4.14 eV and the thickness of the 1%, 2% and 5% of Mn doped CdS thin film were 305,307 and 309 nm respectively. The SEM analysis showed the formation of agglomerated nanoparticle and the particles were uniformly distributed on the surface of the substrate. The average size of Mn doped CdS was found to be 40 nm from the micrograph. The FT-IR analysis of Mn^{2+} doped CdS nanoparticles were in the range of 400-4000 cm^{-1}. The strong and weak absorption peaks were at 1560 and 1629 cm^{-1} are due to CO_2 absorbed on the surface of particles.

Introduction

Cadmium sulphide (CdS) is a II–VI wide direct band gap semiconductor with such applications as thin film solar cells, photo-detectors, transistors, and light emitting diodes [1]. The high transmittance and moderate band gap (2.42 eV) possessed by CdS make it suitable as an ideal material for the fabrication of solar cells especially as an efficient window layer [2]. However, the higher resistivity of as-deposited CdS thin films (of the order of 10^6–10^7 Ω cm) limits its application as an efficient window layer for solar cell fabrication [3]. For this reason, it is very important to control the resistivity of pure CdS, which can be achieved through doping. It has been reported earlier that the optical and electrical properties of CdS thin films can be altered by doping it with metallic ions such as Mg^{2+} [1], Zn^{2+} [4], Cu^{2+} [5], Fe^{2+} [6], Co^{2+} [7], etc. having ionic radii smaller than that of the host ion Cd^{2+}. CdS is a II–VI metal chalcogenide semiconductor intensively investigated over the years because of its application in optoelectronic. Cadmium sulfide (CdS) is commonly employed as n-type, window layer for $Cu(InGa)Se_2$ and CdTe-based solar cells. Cadmium Sulphate (CdS) is one of the most important semiconductors having bulk band gap of 2.42 eV at room temperature and exciton Bohr radius of 5.8 nm. CdS is preferred due to its compact crystallographic cell and electronic affinity. Cadmium Sulphate is also used in the production of solar cells where it is used as a buffer layer in the manufacture of CIGS (Copper -Indium-Gallium-Selenide) solar cells. The most commonly used transition metals for doping are Germanium, Arsenic, Silicon,

Bismuth, Antimony, Phosphorous, Aluminium and Manganese. The doping of transition metals (such as Mn, Fe, Co, Ni) into II – VI semiconductors has led to unique optical, electrical, chemical and mechanical properties which cannot be found in undoped materials. In this present work, Manganese (Mn) is doped with Cadmium Sulphate (CdS).Manganese is the fifth most abundant metal in the Earth's crust and its minerals are widely distributed. Manganese (Mn) plays an important role in a number of physiological processes as a constituent of multiple enzymes. The introduction of Mn into CdS may create a high absorption coefficient and could be employed as widow materials in various photo-thermal and optoelectronic devices. The effect of Mn doping into CdS lowers the resistivity and increases high optical transmittance. Mn increases the electrical resistivity of CdS. Mn doped CdS thin films are promising candidates in the field of photovoltaic energy conversion and are building blocks for spintronics, non-volatile memory and magneto-optical devices. *Caglar* (2006) determined that Mn doped CdS were synthesised by Chemical Bath Deposition method. *Salayar and Patino* (2006) revealed that the effect on the CdS film deposited by Chemical Bath was studied and compared under three deposition conditions like substrate oscillation, magnetic agitation and without agitation. Therefore, in this work we prepare Mg doped CdS thin films by a simple method and characterizes the structural, optical properties. Results were obtained from XRD, UV–Vis, AFM, SEM, and were discussed in this work.

Experimental Details

The chemical bath deposition (CBD) process is a simple, inexpensive and convenient technique for deposition of thin films in solar cells. The present work was carried out by CBD method for single, double and multilayer thin films. An exterior bath, heated by a hot plate, was used to evenly distribute the temperature around a 1000ml deposition beaker. Samples were held vertically by Teflon clamps and were stirred using magnetic stirrer. A glass substrate was used for all layers of deposition. Once the deposition took place, the samples were cleaned with acetone solution.

The experimental set up of chemical bath deposition is shown in Fig. (1). In CBD method, deposition of metal chalcogenide thin film occurs when the substrate is maintained in contact with a dilute chemical bath containing metal and chalcogen ions [8]. The quality of the surface is the most important requirement of a substrate since it is here that the film substrate interaction occurs. The cleanliness of the substrate surface plays a decisive influence on the film growth [9 – 11]. A toughly clean substrate is a prerequisite for the preparation of films with reproducible properties. The choice of cleaning techniques depends on the nature of the substrate, the type of contaminants and the degree of cleanliness required. The process of substrate cleaning requires that bonds are broken between the contaminant's molecules as well as between the contaminant and the substrate. This may be accomplished by chemical means as in solvent cleaning for suitable reagents like aqueous solution of acids and alkalis [12 – 14].
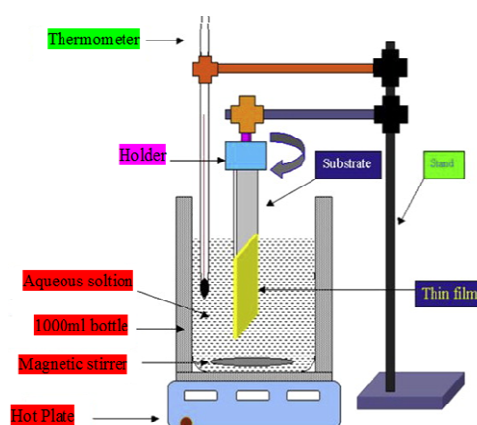

Figure (1) The experimental set up of chemical bath deposition

Solution and precursor for Cadmium Sulphide

Cadmium acetate is used in the chemical bath for the source of cadmium and thiourea is used as a source of sulphur. In a heated aqueous alkaline solution, CdS is grown by the reaction between cadmium salt (Cd (CH$_3$COO)$_2$), thiourea (SC(NH$_2$)$_2$), and aqueous ammonia (NH$_4$OH), with ammonium salt (NH$_4$CH$_3$COO) as a buffer. From the cadmium source, the main chemical equilibrium is involved in the formation of either CdS films or colloids as follows from equation(1- 7).
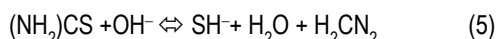
$$NH_4^+ + OH^- \Leftrightarrow NH_3 + H_2O \qquad (1)$$

$$Cd^{2+} + 4NH_3 \Leftrightarrow Cd(NH_3)_4^{2+} \qquad (2)$$
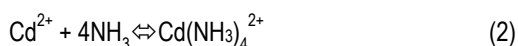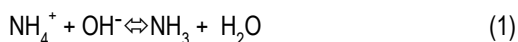
The presence of ammonium salt, however, promotes the forward reaction in eq. (3). This in turn reduces the pH, or OH$^-$ concentration in the reaction bath according to the relation:

$$pH = pK_a + log([NH_3]_0 / [NH_4^+]_0) \qquad (3)$$

Here, [NH$_3$]$_0$ and [NH$_4^+$]$_0$ are the initial aqueous ammonia and ammonium salt concentrations respectively, and pK$_a$ is reported to be 9.2 at 25°C. As a result, Cd^{2+} is predominantly used to form cadmium tetra ammine complex ions (Cd(NH$_3$)$_4^{2+}$), especially if NH$_3$concentration is sufficiently high. These ensure that the product of [Cd^{2+}] and [OH$^-$] is less than the solubility product of Cd (OH)$_2$ (1.2 x 10^{-14}) and prevent the equilibrium reaction.

$$Cd^{2+} + 2 OH^- \Leftrightarrow Cd (OH)_2 (s) \qquad (4)$$
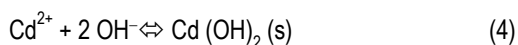
For CdS colloid formation we have, in addition to Eq. (3) and (4),

$$(NH_2)CS + OH^- \Leftrightarrow SH^- + H_2O + H_2CN_2 \qquad (5)$$

$$SH^- + OH^- \Leftrightarrow S^{2-} + H_2O \qquad (6)$$

$$and\ Cd^{2+} + S^{2-} \Leftrightarrow CdS \qquad (7)$$

Finally, the cadmium and sulphur ions react with the ITO substrate and form thin films. The pH is maintained at 8 and the temperature of the bath is maintained at 80ºC.

Preparation of Mn doped CdS thin films

In the CBD method, to prepare Mn doped CdS thin films, 50 ml of 8.63 mM(1 wt%) Cadmium sulfate (CdSO$_4$ anhydrous) and 1.59 mM Manganese chloride (MnCl$_2$ anhydrous) were dissolved in 50ml of DI water. The mixture was poured into a beaker which was stirred and heated at 80ºC and the pH of the bath was maintained between 9 and 10 by adding ammonium hydroxide solution. The deposition was run over 3hrs and thus CdS was deposited on glass substrate.

The process was repeated for 2 wt% and 5wt% of MnCl$_2$. The Mn doped CdS glass slides were cleaned using isopropyl alcohol, chromic acid and soap solution for about 20 minutes and they were washed in deionised water. Finally Mn doped CdS coated thin films were annealed at 300°C for 1 hr in the muffle furnace. The prepared, films were used for further characterization process.

Characterization of thin Films

Mn doped Cds were prepared by chemical bath deposition technique and the films were portrayed by X-ray diffraction, UV–Vis, SEM. The structural parameters were identified and the crystalline nature of the films was confirmed by X-ray diffraction patterns.

The morphology of the thin films was studied using SEM technique and the change in the morphologies due to doping is evident from the images. To resolve the band gap of the material of the thin films after doping, UV–Vis absorption spectra have been recorded using UV–Vis spectrophotometer. It is found that the band gap has been tuned due to doping.

Results and Discussion
X – Ray Diffractometer

The structure of the deposited Mn doped Cds film was confirmed by Powder X-ray diffractometer using CuKα (λ=1.5406Å) within the 2θ range 10-80°. It has a

main peak at 28.32° corresponding to the (2 4 0) plane. The peak position is in accordance with the Mn doped CdS. The lattice parameter of the pure CdS [(Monoclinic) a = 14.31 Å; b = 14.07 Å c = 14.56 Å] are also in accordance with the reported value (JCPDS card # 47-1179). Fig. (2) shows 1 wt% of Mn doped CdS. The films are found to be amorphous in nature. Fig. (3) and Fig. (4) of 2 wt% and 5% shows that Mn doped CdS thin films exhibit polycrystalline behavior. The Bragg's angle for Mn doped CdS shows small shift in the peak position attributed to the local vacancies in the crystal structure.

According to Vegard's law, the dopant alone cannot generate an individual peak by the side of host peak but it can produce adequate shift in the position of host peak. It was understood that the host has accommodated Mn^{2+} ions into its lattice, since Mn^{2+} possesses smaller ion radii 0.66 Å than Cd^{2+} 0.97 Å. The further small shifts in the peak positions in Mn doped CdS nanoparticles ascertain the incorporation of Mn^{2+} into the CdS lattice and also exhibits zero alteration in the phase property of CdS. Further, the electro-negativities of both cations differ with sulfur, (1.55 for Mn, 1.69 for Cd, Pauling Scale) thereby suggesting that Mn gets incorporated into the CdS lattice at vacancy sites most probably. The crystallite size is determined using full width at half maximum (FWHM) of the diffraction peaks using Debye Scherrer's equation,

$$D= \frac{0.9\,\lambda}{\beta\,Cos\,(\theta)}$$

Where **D** is the grain sizes, **β** is the FWHM of the diffraction peak, **θ** is the Bragg diffracting angle, **λ** is the wave length of X-rays and **d** is an inter planar spacing.
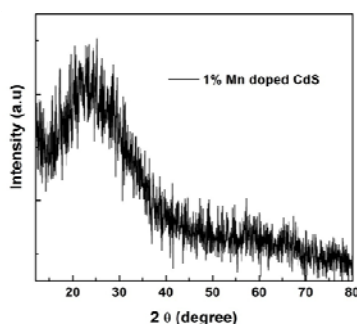

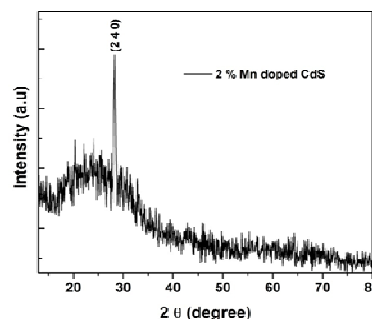**Fig. (2) XRD pattern for 1% Mn doped CdS**

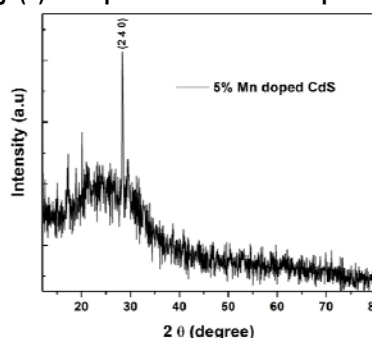**Fig. (3) XRD pattern for 2% Mn doped CdS**

Fig. (4) XRD pattern for 5% Mn doped CdS

Morphological Study

Scanning Electron Microscopy was used for the morphological study of Mn doped CdS thin films. The SEM image for CdS doped with 1 wt% of Mn showed the formation of agglomerated nanoparticles as shown in Fig. (5). For 2%, as shown in Fig. (6) The growth of agglomerated nanoparticles in different shape and orientation may be attributed to controlled nucleation growth during the deposition of nanoparticles on the silica glass substrates. The SEM image of 5 wt% of Mn is clearly shown in Fig. (7) It is observed that the particles are uniformly distributed on the surface of the film. The Mn atoms may have disturbed the growth process resulting in the formation of agglomerated nanoparticles. The magnification results of the SEM image for Mn doped CdS showed a variation from 2μm to 10μm. The average size of Mn doped CdS was found to be 40 nm from the micrograph.
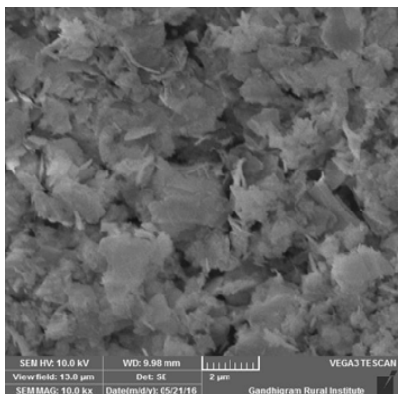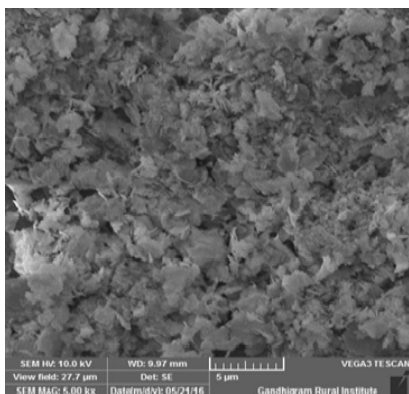
Fig. (5) SEM image for 1% Mn doped CdS

Fig. (6) SEM image for 2% Mn doped CdS
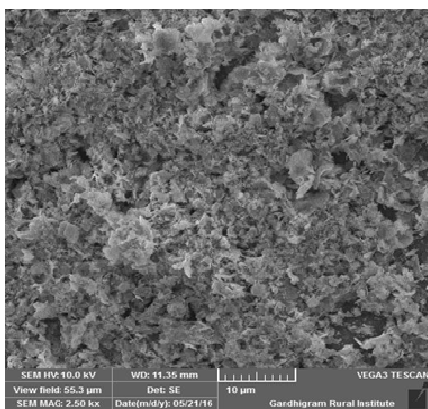

Fig. (7) SEM image for 5% Mn doped CdS

Optical Properties

The optical properties of the single layer thin films were carried out by recording UV-absorption spectra. The spectra for each thin film of Mn doped CdS was recorded using UV-Vis-IR spectrophotometer (Thermo Fischer Helios Alfa) in the range of 200–900 nm. Fig. (8) shows the absorption vs. wavelength spectra. Better absorption was observed in Mn doped CdS thin films in the ultraviolet (UV) and infrared (IR) regions. The transmittance was clearly observed for different percentages of Mn doped CdS in grown in the Fig. (9). The tauc plot of absorption coefficient squared $(\alpha h v)^2$ versus photon energy (hv) of Mn doped CdS thin films are shown in Fig. (10).

The optical transition of the thin films is direct and allowed transition. The thickness of the 1%, 2% and 5% of Mn doped CdS thin films were 305, 307 and 309nm respectively. Transmission studies were used to determine the thickness (t) of the thin films and reflectance to study the refractive index (n) and extinction coefficient of the thin films. These results are tabulated in Table (1).
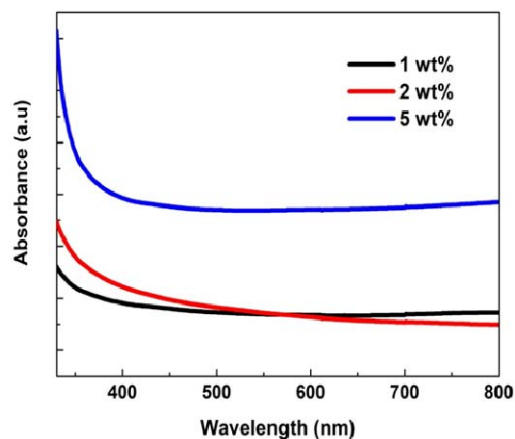

Fig. (8) Typical absorption spectrum of Mn doped CdS thin film for 1%,2% and 5%
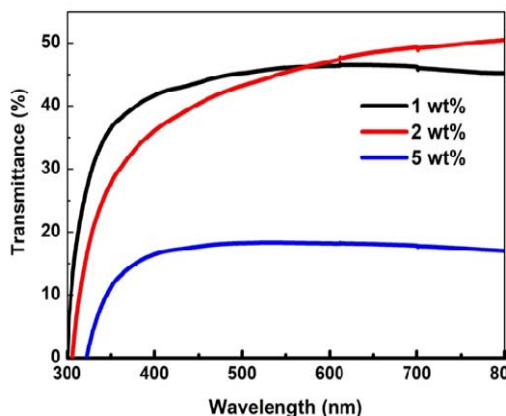
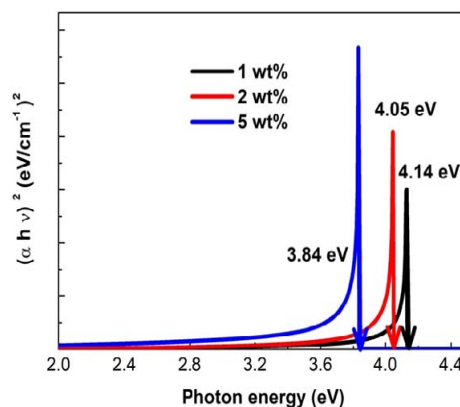**Fig. (9) Transmittance spectrum of Mn doped CdS thin film for 1%,2% and 5%**

Fig. (10) Energy band gap of Mn doped CdS thin film for 1%,2% and 5%

Table.1: Structural and Optical Parameters of Mn doped CdS thin films

Mn doping Wt%	2θ (degree)	FWHM (β) (degree)	D (nm)	Band gap (eV)	Thickness (t) (nm)	Refractive index (n)
1%	-	-	-	4.14	305	2.28
2%	28.32	0.478	17.91	4.05	307	3.86
5%	28.33	0.209	40.96	3.80	309	3.00

FT-IR analysis

Fig. (11) shows FTIR spectra of Mn^{2+} doped CdS nanoparticles in the range of 400–4,000 cm^{-1}. The absorption band at 3,471 cm^{-1} in the spectra is due to the O–H stretching vibration band of H_2O absorbed on the surface of the sample and a small narrow band at 2,945 cm^{-1} indicates the presence of CH_2 stretch bond. The band at 621 cm^{-1} is due to C–S stretching bond and bonds at 540 and 480 cm^{-1} are stretching bond of Cd–S. It was also observed that for CdS nanoparticles doped with Mn^{2+}, the corresponding absorption bands are broad and shifted due to the interaction between OH- group of CdS nanoparticles. The weak absorption peak appears at 654 cm^{-1} due to Mn–S vibration. It is shown that some Cd^{2+} ions have been replaced by Mn^{2+} ions in the cationic sites of CdS particles.
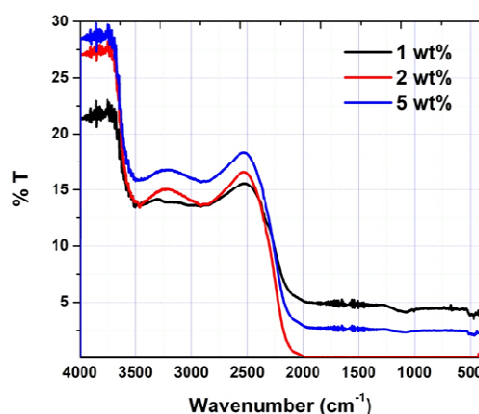

Fig. (11) FT-IR spectra of the Mn doped CdS thin film for 1%,2% and 5%

The additional weak bands observed at 2,340–2,360 and 1,637 cm^{-1} were due to S–H and H–O–H bending. A

medium strong band due to stretching vibrations of sulfide was observed at 1,415 cm^{-1} in all the spectra. The absorption band appeared about at 3,458 cm^{-1} was assigned to stretching vibration of the O–H group arising from the water vapor adsorbed by the samples. The strong and weak absorption peaks centered at 1,560 and 1,629 cm^{-1} were attributed to CO_2 adsorbed on the surface of the particles. In fact, adsorbed water and CO_2 are common to all powder samples exposed to atmosphere and are even more pronounced for nano sized particles with high surface area.

Conclusion

The transition metal Mn doped CdS were successfully synthesized by Chemical Bath Deposition method. The Structure of the deposited Mn doped CdS was confirmed by Powder

X-ray diffractometer. It has a main peak at 28.32° corresponding to the (2 4 0) plane. The crystalline size determined using full width half maximum (FWHM) of the diffraction peaks using the Debye Scherrer's equation. The Mn doped CdS thin films are found to be amorphous in nature. The UV-Vis-IR studies reveal that Mn doped CdS thin film was in the range of 200-900 nm. The Optical band gap was found to be 3.84 eV-4.14 eV and the thickness of the 1%, 2% and 5% of Mn doped CdS thin film were 305,307 and 309 nm respectively. The SEM analysis showed the formation of agglomerated nanoparticle. It was observed that the particles were uniformly distributed on the surface of the substrate. The average size of Mn doped CdS was found to be 40 nm from the micrograph. The FT-IR analysis of Mn^{2+} doped CdS nanoparticles were in the range of 400-4000 cm^{-1}. The strong and weak absorption peaks were at 1560 and 1629 cm^{-1} are due to CO_2 absorbed on the surface of particles.

Reference

1. T. Sivaraman, A.R. Balu, V.S. Nagarethinam. Effect of magnesium incorporation on the structural, morphological, optical and electrical properties of CdS thin films. Mater. Sci. Semicon. Proc., 27 (2014), pp. 915-923.
2. R. Mendoza-Perez, J. Sastre Hernandez,G. Puente, O. Vigil-Galan CdTe solar cell degradation studies with the use of CdS as the window material Sol. Energy Mater. Sol. Cells, 8 (2009), pp. 79-84
3. J. Hiie, T. Dedova, V. Valdna, K. Muska Comparative study of nano-structured CdS thin films prepared by CBD and spray pyrolysis: annealing effect. Thin Solid Films, 511–512 (2006), pp. 443-447
4. M. Anbarasi, V.S. Nagarethinam, A.R. Balu. Investigations on the structural, morphological, optical and electrical properties of undoped and nano sized Zn-doped CdS thin films prepared by a simplified spray technique Mater. Sci. Pol., 32 (2014), pp. 652-660
5. N.A. Shah, R.R. Sagar, W. Mahmood, W.A.A. Syed. Cu-doping effects on the   physical properties of cadmium sulfide thin films J. Alloys Compd., 512 (2012), pp. 185-189
6. N. Badera, B. Godbole, S.B. Srivastava, P.N. Vishwakarma, L.S. SharathChandra, D. Jain, M. Gangrade, T. Shripathi, V.G. Sathe, V. Ganesan Quenching of photoconductivity in Fe doped CdS thin films prepared by spray pyrolysis technique
7. S.T. Mane, P.C. Pingale, R.V. Suryawanshi, V.S. Karande, L.P. Desmukh, M. SharonOn the surface morphology and transport properties of chemical bath deposited CoxCd1-xS thin films: a correlation Electrochim. Acta, 114 (2013), pp. 494-499.
8. Issaial O.Oladeji, et,al., (1997) "Optimization of Chemical bath deposited Cadmium Sulphide Thin

films" Journal of Electrochemistry Society, Vol.144 (7).

9. K. Wasa, et. al., (2004) thin film material Technology, Spinger.

10. D. Glocker, et al., (2000) "Handbook of Thin Film Process Technology 99/1 Substrate Preparation for Thin Film Deposition" McGraw-Hill, New York.

11. JamesG.Speight, (1988) "Synthetic Fuels Handbook of Properties, Process, and Performance" McGraw Hill Hand book. CRC Press, New York.

12. D.J.Stirland and R.W.Bicknll, (1959) "Studies of the Structure of Anodic Oxide Films on Aluminum", Journal of Electrochemical society, 106:481.

13. M.L.Levin, (1958) "The formation of crystalline anodic oxide films on beryllium" Transaction Faraday Society, 54:935.

14. J.G.Gualtieri, et. al., (1963) "Laser reflectogram method for the study of crystal surfaces and epitaxial deposits" Review science Instruments, 34:108.